WHEAT STRAW PYROLYSIS ANALYSIS BY THERMOGRAVIMETRY AND GAS CHROMATOGRAPHY–MASS SPECTROMETRY

QING YANG and SHUBIN WU

State Key Laboratory of Pulp Paper Engineering, South China University of Technology, Guangzhou, Guangdong 510640, P. R. China

Received November 20, 2008

The effect of the heating rates and the existence of a Ni-catalyst on the thermogravimetric characteristics of wheat straw were investigated by thermogravimetry and gas chromatography–mass spectrometry. The weight loss of wheat straw was not markedly influenced by the heating rates, over a temperature range from 220.6 to 391.2 °C, although, to obtain the same weight loss, the corresponding temperature was increased and the heating rates were enhanced. The thermogravimetric kinetic parameters of wheat straw were calculated both without catalyst and with 0.5% Ni-catalyst, by the method of Kissinger; the apparent activation energy values of wheat straw were of 93.92 and 119.80 KJ·mol^{-1}, and the frequency factors *lnA* were of 17.82 and 23.02 min^{-1}, respectively. The weight loss of wheat straw was not markedly influenced by the Ni-catalyst, while pyrolysis–gas chromatography–mass spectrometry (Py-GC-MS) evidenced that, at 800 °C, the presence of the catalyst influenced the peak intensities derived from cellulose, hemicellulose and lignin. It was concluded that the Ni-catalyst favors a more catalytic effect on wheat straw lignin, that is, the total value of the peak area from phenolic compounds and vanillin was higher than that from furfural and levoglucosan.

Keywords: wheat straw, thermogravimetry, kinetics, Py-GC-MS, catalyst, pyrolysis

INTRODUCTION

Recently, extensive research, aiming at developing renewable energy resources from biomass, has been carried out, especially, the pyrolysis of biomass by the Pyrolysis Network (PyNe).[1,2] Processes such as combustion, gasification and pyrolysis have been identified as possible routes for energy and transport fuel production. Pyrolysis, basically a polymeric structure cracking process, converts the lignocellulosic materials into a volatile fraction char. The volatile fraction (gas or liquid, depending on its molecular weight) can be used as both fuel and chemical synthesis source. On the other hand, the solid fraction presents several applications, such as domestic fuel, for the production of activated carbon, or as reducing agent in metallurgy.[3] Hsisheng[4] and Raveendran[5] investigated the effect of alkali and other metals on the decomposition behavior of biomass. The researches carried out indicated[6,7] that a small amount of certain metallic elements present in the biomass had a significant catalyzing influence on pyrolysis and very good catalysis effects, so that even a low content visibly increased the reaction rate and affected the generation of a three-phase product. All these observations suggest that the inorganic species present in biomass become decisive factors, determining the biomass behavior under thermal degradation which, in turn, affects the quality and conversion during pyrolysis, combustion and gasification.

Wheat straw, which is a common biomass raw material, was subjected to pyrolysis, which permitted a deep understanding of its reaction process and mechanism; further on, the effect of the Ni-catalyst on wheat straw during pyrolysis was investigated by analyzing the influence factors and the dynamics of the raw material during thermal

decomposition, which provided the basic theoretical data for the newly-applied pyrolysis technique of biomass, promoted by the new technical advances.

EXPERIMENTAL

Samples

Wheat straw, collected from the Baoding region (Hebei Province), was milled to pass a 120 mesh and extracted for elemental, thermogravimetry and Py-GC-MS analyses. The Ni-catalyst, provided by Lanzhou Petroleum Chemical Research Institute (Gansu Province), was nickel, a metallic chemical element with the symbol Ni and atomic number 28. As a silvery-white, high-polished metal, it belongs to transition metals and is hard and ductile. Similarly with the massive forms of chromium, aluminum and titanium, nickel is a very reactive element, although it reacts slowly in air at normal temperatures and pressures. The most common oxidation state of nickel is +2, when Ni complexes are observed. It is also thought that a +6 oxidation state may exist, however, results are inconclusive.

Elemental analysis

The analysis of wheat straw elements was implemented in a Vario-I elemental analyzer and an ICP inductively coupled plasma emission spectrometer. Measurement parameters:

- Oxidation furnace temperature: 1150 °C;
- Reduction furnace temperature: 850 °C;
- Carrier gas flow rate of the measuring cell: 90 mL/min;
- Carrier gas flow rate of the reference cell: 20 mL/min;
- Oxygen flow rate: 30-80 mL/min.

ICP sample dissolution was infrared digestion in perchloric acid and concentrated nitric acid, at 100 °C (digestion conditions).

Thermogravimetric analysis

Thermogravimetric experiments were performed in a TG209 Integrated Thermal Gravimetric Analyzer (NETZSCH Co., Germany), with high-purity nitrogen as a carrier gas, at a flow rate of 40 mL/min. About 6-12 mg samples were put in a ceramic crucible each time, while samples both without catalyst and with 0.5% Ni catalyst were heated from room temperature to 800 °C, at heating rates of 10, 20, 30, 40 and 50 °C/min, respectively. The sample with 1% Ni-catalyst was also tested under the above-mentioned conditions, at a heating rate of 30 °C/min. The amount of Ni-catalyst used was based on the absolute dry content of wheat straw. The calculated thermogravimetic rate data were automatically output through an TG209 Integrated Thermal Gravimetric Analyzer system. The thermogravimetric experiment was applied to obtain the parameters of chemical dynamics, so that the influence of any error was reduced as much as possible. The average size of all samples was below 0.2 mm, so that the weight loss of the samples was under the control of the kinetic reaction.

Py-GC-MS analysis

Py-GC-MS analysis was carried out on a combined system of an American CDS5150 pyrolyzer and Shimazu QP2010 Plus GC-MS. The pyrolysis temperature was set at 800 °C, heating time = 1 min. GC qualitative analysis was conducted with a DB-Wax fused silica capillary column (30 m × 0.25 mm, *i.e.* film thickness = 0.25 μm); He flow rate = 1.22 mL/min; column temperature was held at 50 °C for 5 min, then raised to 280 °C at a rate of 10 °C/min; injector temperature = 250 °C; EI-MS scan range = 45-600 amu, scan time = 0.5 s; EI ionization energy = 70 eV.

Table 1
Analysis of wheat straw organic elements

Organic elements content, wt/%				
C	H	O*	N	S
42.50	7.26	50.04	0.06	0.14

O* – by difference

Table 2
Analysis of wheat straw inorganic elements

Inorganic elements content, ppm				
Al	Ca	K	Zn	Mn
84.30	2443.52	1196.08	9.92	10.92
Cu	Cd	Fe	Mg	Na
16.65	4.34	370.85	882.48	209.00

RESULTS AND DISCUSSION

Influence of heating rates on the thermogravimetric curve of wheat straw

Figures 1 and 2 plot the thermogravimetric curves of wheat straw at different heating rates (10, 20, 30, 40 and 50 °C/min). When temperature increases from 220.6 to 391.2 °C, the weight loss of wheat straw is not influenced by the heating rates; the residue weight of wheat straw at 391.2 °C is 36.2 (wt/%) for the different heating rates shown in Figure 1. Figure 2 illustrates the maximum value reached by the thermogravimetric rate over the 220.6~400.3 °C temperature range; the peak of both thermogravimetric and differential thermogravimetric curves shifted towards a high temperature region, the temperatures corresponding to the maximum weight loss, at different heating rates, being of 323.3, 345.6, 349.5, 364.4 and 372.2 °C, respectively.

However, at a temperature above 391.2 °C, the thermogravimetric law was not essentially affected by the heating rates of 20 °C/min or higher, although maximum weight occurred at a heating rate of 10 °C/min; it was observed that, at a given temperature of the same sample, the slower heating rates, the higher the degradation degree. Yang *et al.*[8] reported that hemicelluloses started the decomposition easily, weight loss occurring mainly at 220~315 °C, while cellulose pyrolysis appeared at higher temperatures (315~400 °C), and the hemicelluloses and cellulose of wheat straw were disintegrated, to a certain extent, between 220.6 and 391.2 °C (Fig. 1). Song *et al.*[9] reported that lignin pyrolysis occurred evidently at about 160 °C, over a wide range. Figure 1 shows that the thermogravimetric curve of wheat straw was flat at temperatures over 550 °C.

Catalyst influence on the thermogravimetric curve of wheat straw

The influence of different catalyst dosages on the thermogravimetry of wheat straw, at a heating rate of 30 °C/min, was plotted separately in Figures 3 and 4.

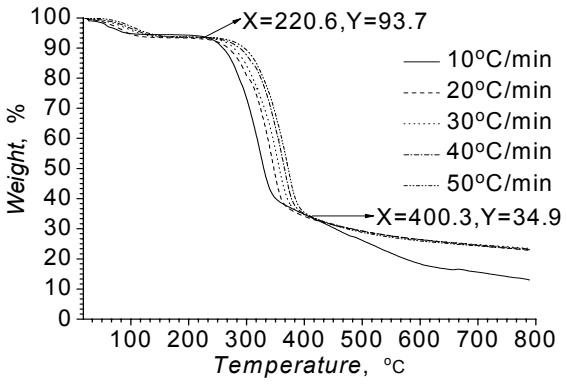

Figure 1: TG curves of wheat straw at different heating rates

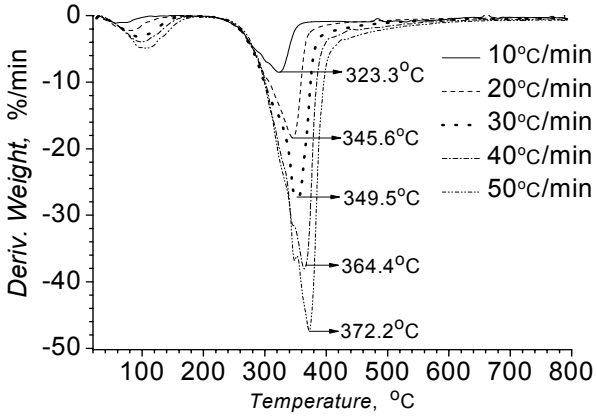

Figure 2: DTG curves of wheat straw at different heating rates

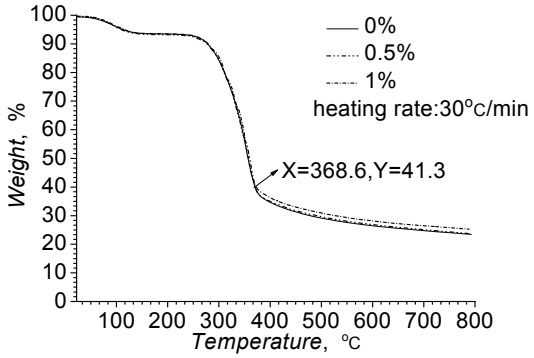

Figure 3: TG curves of wheat straw at different catalyst dosages

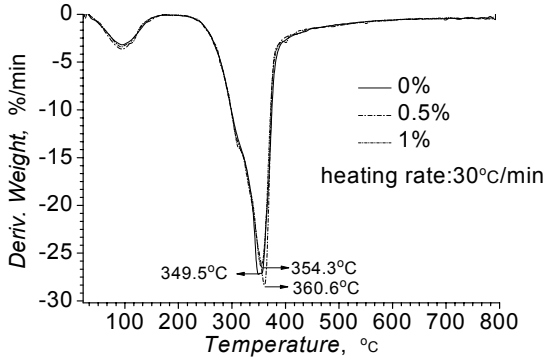

Figure 4: DTG curves of wheat straw at different catalyst dosages

Catalytic thermogravimetric analysis of wheat straw was carried out by adding a given amount of Ni-catalyst. Figure 3 shows that the weight loss of wheat straw was not markedly influenced by the Ni-catalyst. However, at temperatures over 368.6 °C, the curve with 1% Ni-catalyst deviated slightly from the other two curves. The maximum temperature, in the presence of the catalyst mildly drifted towards a high-value range.

Kinetics of wheat straw pyrolysis

The kinetic study of biomass pyrolysis was especially important, once it constituted the initial step of combustion and gasification processes. Knowledge on the thermal decomposition kinetics of lignocellulosic materials was useful in designing gasifiers and pyrolysis reactors. The method of Kissinger, viewed as a sort of non-isothermal kinetics, benefiting from fast measurements, wide temperature range and large utilizations, was applied in the experiment.

The experimental data were used to fit the kinetic model (eq. 1):

$$\frac{d\alpha}{dt} = kf(\alpha) \qquad (1)$$

where

$$a = 1 - \frac{m_{(t)} - m_f}{m_0 - m_f} \text{ and } k = A\exp(-E/RT)$$

$m_{(t)}$ was the experimental weight at each monitoring time, m_f was the final weight, and m_o was the initial dry mass. $f(\alpha)$ was the differential form kinetic mechanism function and k was the kinetic constant which, according to Arrhenius equation, was a function of the pre-exponential factor (A), apparent activation energy (E), absolute temperature and constant of ideal gas law (R).

The temperature-time relation was computed from the following expression (eq. 2):

$$T = T_o + \beta t \qquad (2)$$

where β was the constant heating rate (°C/min), and T_o – the initial temperature. The function (eq. 3) was deduced from eqs. 1 and 2, as follows:

$$\ln\left(\frac{\beta}{T_p^2}\right) = -\frac{E}{RT_P} + \ln\left(\frac{AR}{E}\right) \qquad (3)$$

Eq. 3 provided the formula for calculating[10] the apparent activation energy (E) and the constant of ideal gas law (R) of Kissinger.

While the temperature reached its maximum, the effect of the heating rates on the peak temperature followed eq. 3. The peak temperature and heating rates given in Figures 2 and 5 are shown separately in Tables 3 and 4.

The graphing of $\ln(\beta/T_p^2)$ to $1/T_P$ is shown in Figures 6 and 7.

The equation was fit into Figure 6 as:

$$y = -11.2966 \times 10^3 + 8.4842 \quad (4)$$

The linear regression coefficient (R^2) was 0.99, the slope was -11.2966×10^3, from which the apparent activation energy (E), of 93.92 KJ/mol, was deduced; the intercept of the fit equation was 8.4842, and the pre-exponential factor (lnA) equaled 17.82 min^{-1}.

The equation was fit into Figure 7 as:

$$y = -14.4093 \times 10^3 + 13.4409 \quad (5)$$

The linear regression coefficient (R^2) was 0.99 and the slope was -14.4093×10^3, from which the apparent activation energy (E), of 119.80KJ/mol, was deduced; the intercept of the fit equation was 13.4409, so that the pre-exponential factor (lnA) equaled 23.02 min^{-1}.

Py-GC-MS analysis of wheat straw

To further investigate the influence of Ni-catalyst on pyrolysis, Py-GC-MS analysis was performed, both without catalyst and with 1% Ni-catalyst, at 800 °C. The total Py-GC-MS ion-current spectrograms of wheat straw, without catalyst and with 1% Ni-catalyst, at 800 °C were shown in Figures 8 and 9.

Table 3
Parameters of Kissinger formula (no catalyst)

β/(min^{-1})	T	$1/T \times 10^{-3}$	$1/T^2 \times 10^{-6}$	$\beta/T^2 \times 10^{-6}$	$\ln(\beta/T^2 \times 10^{-6})$
10	596.3	1.68	2.82	28.2	-10.48
20	618.6	1.62	2.62	52.4	-9.86
30	622.5	1.61	2.59	77.7	-9.46
40	637.4	1.57	2.46	98.4	-9.23
50	645.2	1.55	2.40	120.0	-9.03

Table 4
Parameters in Kissinger formula (0.5% Ni-catalyst)

β/(min^{-1})	T	$1/T \times 10^{-3}$	$1/T^2 \times 10^{-6}$	$\beta/T^2 \times 10^{-6}$	$\ln(\beta/T^2 \times 10^{-6})$
10	603.3	1.66	2.76	27.6	-10.50
20	618.8	1.62	2.62	52.4	-9.86
30	633.6	1.58	2.50	75.0	-9.50
40	634.3	1.57	2.47	98.8	-9.22
50	641.9	1.56	2.43	121.5	-9.02

Tables 5 and 6 show the chemical identity of the pyrolysis products, both without catalyst and with 1% Ni-catalyst, at 800 °C.

A comparison of Figures 8 and 9 indicates the effect of Ni-catalyst on wheat straw during pyrolysis. Laevoglucose, furfural and vanillin, three important chemical products, were present during thermal decomposition, evidencing the catalytic impact on the pyrolysis of the three kinds of main components.

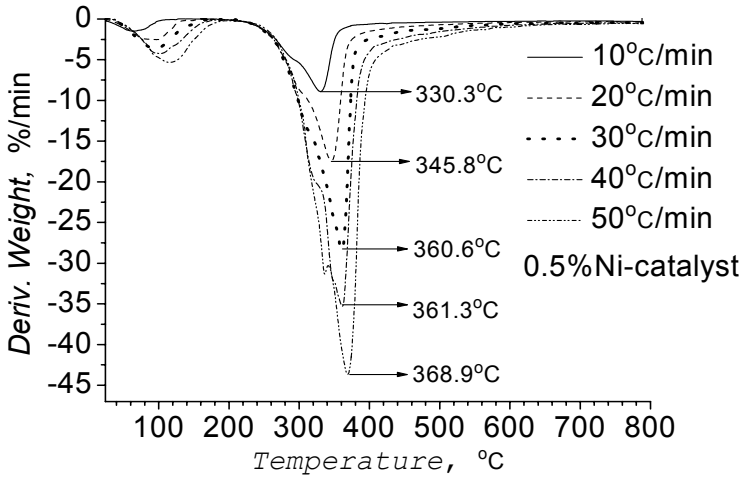

Figure 5: DTG curves of wheat straw with 0.5% Ni-catalyst at different heating rates

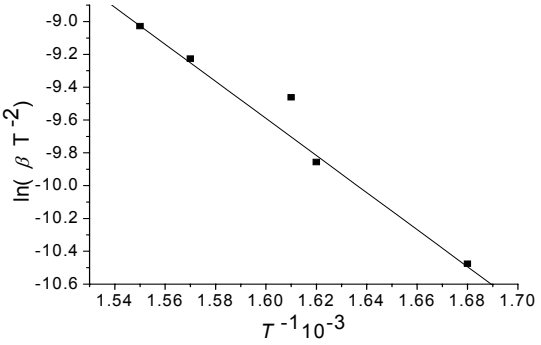

Figure 6: Linearization curves of Kissinger method (no catalyst)

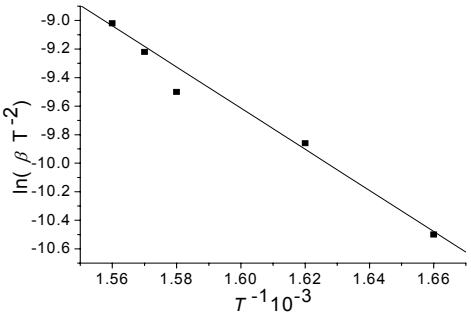

Figure 7: Linearization curves of Kissinger method (0.5% Ni-catalyst)

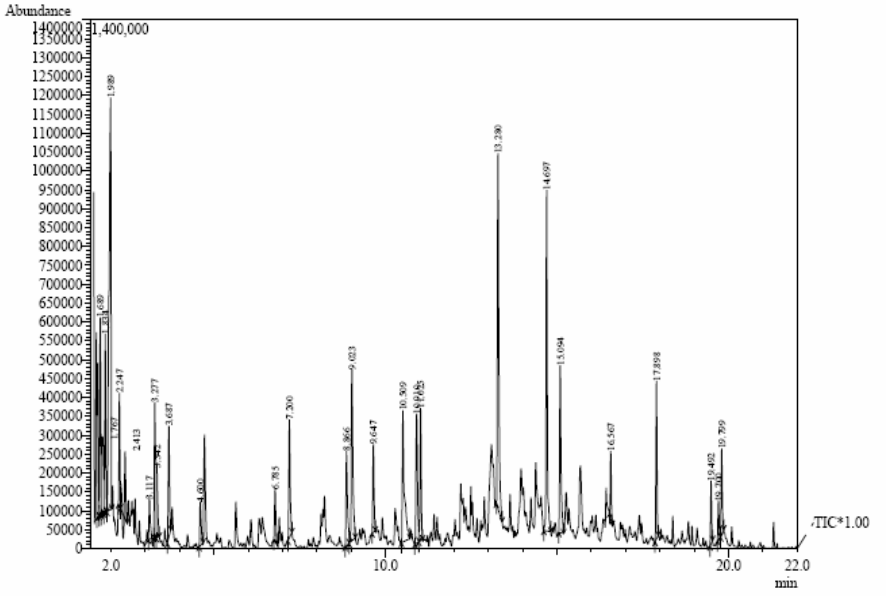

Figure 8: Py-GC-MS ion-current spectrogram of wheat straw without catalyst, at 800 °C

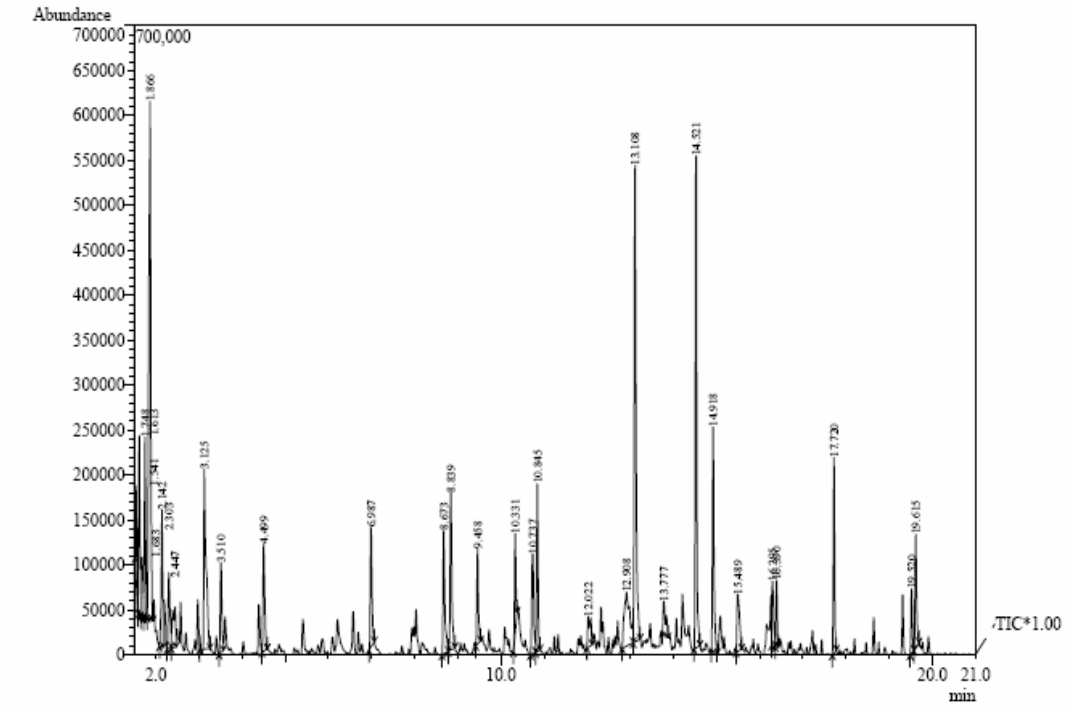

Figure 9: Py-GC-MS ion-current spectrogram of wheat straw with 1% Ni-catalyst at 800 °C

Table 5
Chemicals identified by Py-GC-MS without Ni-catalyst

Peak	Retention time (min)	Compound	Relative percentage content* (%)	Formula
1	1.617	Butadiene	3.32	C_4H_6
2	1.692	2,2-Dimethyl-3-hydroxypropionaldehyde	4.42	$C_5H_{10}O_2$
3	1.767	Ethylidenecyclopropane	2.86	C_5H_8
4	1.833	3-Methylpentanoic acid	3.95	$C_6H_{12}O_2$
5	1.992	Acetic acid	16.64	$C_2H_4O_2$
6	2.417	Benzene	1.58	C_6H_6
7	3.117	2,2'-Bioxirane	0.89	$C_4H_6O_2$
8	3.275	Propanal	3.67	C_3H_6O
9	3.342	1-Hydroxy-2-butanone	1.97	$C_4H_8O_2$
10	3.683	Toluene	2.83	C_7H_8
11	4.600	Cyclopentenone	1.21	C_5H_6O
12	6.783	Cinnamene	1.23	C_8H_8
13	7.200	1,2-Cyclopentanedione	3.20	$C_5H_6O_2$
14	9.025	Phenol	5.51	C_6H_6O
15	9.650	3-Methyl-1,2-cyclopentanedione	2.20	$C_6H_8O_2$
16	10.508	*o*-Methylphenol or *m*-Methylphenol	5.38	C_7H_8O
17	10.908	*p*-Methylphenol	4.28	C_7H_8O
18	11.025	*o*-Methoxyphenol or *p*-Methoxyphenol	3.12	$C_7H_8O_2$
19	13.283	2,3-Dihydrobenzofuran	10.42	C_8H_8O

20	14.700	4-Hydroxy-3-methoxystyrene or 2-Methyl-4-hydroxyacetophenone	8.34	$C_9H_{10}O_2$
21	15.092	1,3-Dimethoxy-2-hydroxybenzene or 3,4-Dimethoxyphenol	4.64	$C_8H_{10}O_3$
22	16.567	Eugenol	1.26	$C_{10}H_{12}O_2$
23	17.900	3,5-Dimethoxyacetophenone	3.34	$C_{10}H_{12}O_3$
24	19.492	2,6-Dimethoxy-4-allylphenol	1.22	$C_{11}H_{14}O_3$
25	19.700	Acetosyringone	0.81	$C_{10}H_{12}O_4$
26	19.800	4-((1E)-3-Hydroxy-1-propenyl) -2-methoxyphenol	1.93	$C_{10}H_{12}O_3$

Relative percentage content* – based on the peak area

Table 6
Chemicals identified by Py-GC-MS with 1% Ni-catalyst

Peak	Retention time (min)	Compound	Relative percentage content* (%)	Formula
1	1.542	Butadiene	1.41	C_4H_6
2	1.617	2,2-Dimethyl-3-hydroxypropionaldehyde	3.41	$C_5H_{10}O_2$
3	1.683	Ethylidenecyclopropane	1.53	C_5H_8
4	1.750	3-Methylpentanoic acid	3.09	$C_6H_{12}O_2$
5	1.867	Acetic acid	13.87	$C_2H_4O_2$
6	2.142	2-Hydroxymethylcyclopropanecarboxylic acid methyl ester	2.83	$C_6H_{10}O_3$
7	2.300	Benzene	1.98	C_6H_6
8	2.450	Propanoic acid	1.72	$C_3H_6O_2$
9	3.125	Propanal	5.52	C_3H_6O
10	3.508	Toluene	1.99	C_7H_8
11	4.500	Furfural	2.61	$C_5H_4O_2$
12	6.983	1,2-Cyclopentanedione	2.73	$C_5H_6O_2$
13	8.842	Phenol	3.71	C_6H_6O
14	9.458	3-Methyl-1,2-cyclopentanedione	1.93	$C_6H_8O_2$
15	10.333	*o*-Methylphenol or *p*-Methylphenol	1.86	C_7H_8O
16	10.733	*m*-Methylphenol or *p*-Methylphenol	2.82	C_7H_8O
17	10.842	*o*-Methoxyphenol or *p*-Methoxyphenol	3.16	$C_7H_8O_2$
18	12.025	3,5-Dimethylphenol or 3,4-Dimethylphenol	1.22	$C_8H_{10}O$
19	12.908	*o*-Hydroxyphenol	4.29	$C_6H_6O_2$
20	13.108	2,3-Dihydrobenzofuran	11.50	C_8H_8O
21	13.775	*p*-(Hydroxymethyl)phenol	1.15	$C_7H_8O_2$
22	14.517	4-Hydroxy-3-methoxystyrene or 2-Methyl-4-hydroxyacetophenone	9.34	$C_9H_{10}O_2$
23	14.917	1,3-Dimethoxy-2-hydroxybenzene or 3,4-Dimethoxyphenol	4.62	$C_8H_{10}O_3$
24	15.492	Vanillin	2.04	$C_8H_8O_3$
25	16.292	Levoglucosan	1.50	$C_6H_{10}O_5$
26	16.392	Eugenol	1.17	$C_{10}H_{12}O_2$
27	17.717	3,5-Dimethoxyacetophenone	3.35	$C_{10}H_{12}O_3$
28	19.517	Acetosyringone	1.21	$C_{10}H_{12}O_4$
29	19.617	4-((1E)-3-Hydroxy-1-propenyl)-2-methoxyphenol	2.42	$C_{10}H_{12}O_3$

Relative percentage content* – based on the peak area

Even more important was that the higher catalytic effect of the Ni-catalyst on the lignin of wheat straw was discovered in various kinds of phenolic compounds (shown in Table 6), such as 3,5-Dimethylphenol or 3,4-Dimethylphenol, o-Hydroxyphenol and p-(Hydroxymethyl)phenol and 3,5-Dimethoxyacetophenone, while the total value of the peak area from phenolic compounds and vanillin was higher than that of furfural and levoglucosan, in the presence of the Ni-catalyst.

CONCLUSIONS

- The weight loss of wheat straw was not influenced by changing the heating rates from 220.6 to 391.2 °C although, at temperatures above 391.2 °C, the thermogravimetric law was not essentially affected by the heating rates.
- The weight loss of wheat straw was not markedly influenced by the Ni-catalyst and by the maximum temperature, in the presence of the catalyst mildly drifted towards a high-value range.
- The Ni-catalyst favors a higher catalytic effect on the lignin of wheat straw, comparatively with cellulose and hemicelluloses.

ACKNOWLEDGEMENT: The investigation was supported by a grant from the Major State Basic Research Development Program of China (973 Program - No. 2007CB210201), from the National High Technology Research and Development Program of China (863 Program - No. 2007AA05Z456), and from the National Natural Science Foundation of China (No. 20576043).

REFERENCES

[1] A. V. Bridgwater, "Fast Pyrolysis of Biomass: A Handbook", Vol. 2, CPL Press, Berks, 2002.
[2] A. V. Bridgwater, "Fast Pyrolysis of Biomass: A Handbook", Vol. 2, CPL Press, Berks, 2005.
[3] M. J. Antal, S. G. Allen, X. Dai *et al*., *Ind*. *Eng*. *Chem*. *Res*., **39**, 4024 (2000).
[4] T. Hsisheng and Y. Chou Wei, *Ind*. *Eng*. *Chem*. *Res*., **37**, 3806 (1998).
[5] K. Raveendran, A. Gansh and K. C. Khilar, *Fuel*, **74**, 1812 (1995).
[6] A. G. W. Bradbury, Y. Sakai and F. Shafizadeh, *J*. *Appl*. *Polym*. *Sci*., **23**, 3271 (1979).
[7] R. Fahmi, A. V. Bridgwater, L. I. Darvell *et al*., *Fuel*, **86**, 1560 (2007).
[8] H. P. Yang, R. Yan, H. P. Chen, C. G. Zheng, D. H. Lee and D. T. Liang, *Energ*. *Fuel*., **20**, 383 (2006).
[9] C. C. Song and H. Q. Hu, *Coal Conversion*, **26**, 91 (2003).
[10] H. F. Kissinger, *Anal*. *Chem*., **29**, 1702 (1957).